

# Journal of Materials Chemistry A

Accepted Manuscript



This is an *Accepted Manuscript*, which has been through the Royal Society of Chemistry peer review process and has been accepted for publication.

*Accepted Manuscripts* are published online shortly after acceptance, before technical editing, formatting and proof reading. Using this free service, authors can make their results available to the community, in citable form, before we publish the edited article. We will replace this *Accepted Manuscript* with the edited and formatted *Advance Article* as soon as it is available.

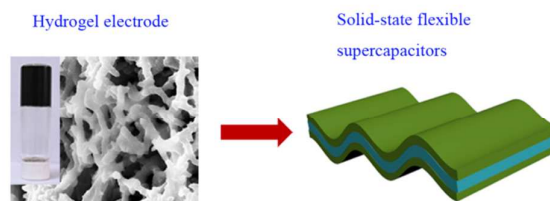
You can find more information about *Accepted Manuscripts* in the [Information for Authors](#).

Please note that technical editing may introduce minor changes to the text and/or graphics, which may alter content. The journal's standard [Terms & Conditions](#) and the [Ethical guidelines](#) still apply. In no event shall the Royal Society of Chemistry be held responsible for any errors or omissions in this *Accepted Manuscript* or any consequences arising from the use of any information it contains.

## Flexible Solid-State Supercapacitors Based on Conducting Polymer Hydrogel with Enhanced Electrochemical Performance

Kai Wang \*, Xiong Zhang, Chen Li, Haitao Zhang, Xianzhong Sun, Nansheng Xu and Yanwei Ma \*

Conducting polymer hydrogels instead of traditional solid materials are used as the electrode materials to prepare high-performance flexible solid-state supercapacitor.



# Flexible Solid-State Supercapacitors Based on Conducting Polymer Hydrogel with Enhanced Electrochemical Performance

Cite this: DOI: 10.1039/x0xx00000x

Received 00th January 2012,  
Accepted 00th January 2012

DOI: 10.1039/x0xx00000x

[www.rsc.org/](http://www.rsc.org/)

Kai Wang \*, Xiong Zhang, Chen Li, Haitao Zhang, Xianzhong Sun, Nansheng Xu and Yanwei Ma \*

In this paper, conducting polyaniline hydrogel instead of traditional solid electrode materials is used as electrode materials to prepare high performance flexible solid-state supercapacitor. Conducting polymer hydrogel combines the properties of hydrogel with the electrical conductivity, thus offering intrinsic porous conducting frameworks and promoting the transport of charges, ions, and molecules. According to our results, the capacitance of polyaniline hydrogel electrode is quite remarkable (430F/g) in this prototype flexible solid-state supercapacitor with two-electrode configuration. Furthermore, this supercapacitor shows excellent rate capability, cyclic stability and bendable performance. Besides, this supercapacitor can drive a glow armband to work very well, which demonstrates the device has great potential to work as power source in the case of real application.

## 1. Introduction

Continuous progress in wearable technologies, especially wearable electronics and photonics device, is creating new products to revolutionize the way of our daily lives.<sup>1, 2</sup> Some wearable gadgets have been demonstrated, including Philips Fluid flexible smartphone, Cutecircuit Galaxy Dress, T-shirtOS, and “Hi-call” Bluetooth enabled phone-gloves. It is noted that all these wearable electronic devices are powered with conventional batteries and capacitors.<sup>3</sup> In order to further facilitate the wearability, the development trend in energy storage system is to light, thin and flexible, while it remains a large challenge to obtain a flexible battery or capacitor with excellent performance currently.<sup>4-6</sup> Innovation in energy storage technologies to explore lightweight and flexible devices is highly demanded.<sup>7, 8</sup>

In various energy storage devices, supercapacitors (also known as electrochemical capacitors) that can quickly store and release electric energy have been used in a variety of applications, such as back-up power systems, electric vehicles, and industrial energy management systems.<sup>9, 10</sup> On the basis of charge-storage mechanism, supercapacitors generally include electrical double-layer capacitors (EDLCs) that store the charge at the electrode - electrolyte interface and pseudocapacitors based on fast and reversible faradaic reactions.<sup>11, 12</sup> Flexible solid-state

supercapacitors hold great promises to be energy storage unit for flexible and wearable electronics, in particular in the case of some wearable electronic devices with high power requirements.<sup>3, 13</sup> Normally, a flexible solid-state supercapacitor is composed of sandwich laminated structure - two stacking flexible solid electrodes and the gel polymer electrolytes in between (Figure 1a).<sup>3, 4</sup> With respect to this structure, only the solid electrode surface can contact with gel polymer electrolytes, which limits the usage of inner electrode materials and further results in low capacitance and poor rate capability.<sup>14</sup> Here, in order to address this issue, we propose a new strategy to use hydrogel materials instead of traditional solid materials as the electrode materials for flexible solid-state supercapacitors (Figure 1b). Hydrogel consists of a solid three-dimensional network and large amounts of water dispersion medium.<sup>15, 16</sup> For hydrogel electrode materials, active materials are swollen with water so that the electrolytes ions are easily diffuse into the inner electrode materials along the water medium under the applied potential.<sup>17-19</sup> Thus, all the electrode active materials can sufficiently contact with electrolyte ions. With this design, the enhanced capacitance and rate performance are expected. As one typical electrode material of pseudocapacitors, the conducting polymers such as polyaniline (PANI) possess advantageous properties, such as low cost, ease to synthesis as well as relatively high conductivity and intrinsic

flexibility.<sup>20</sup> Conducting polymer hydrogel combines the unique properties of hydrogel with the electrical properties, thus offering intrinsic 3D conducting frameworks and promoting the transport of charges, ions, and molecules.<sup>19, 21</sup> In this paper, PANI hydrogel is employed as active electrode materials to construct a symmetric flexible solid-state supercapacitor. The experiment results demonstrate the as-prepared flexible device possess superior electrochemical performance and flexibility.

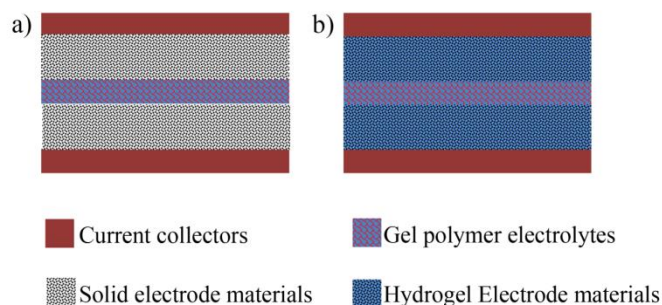


Figure 1 The configuration of a traditional solid-state flexible supercapacitor (a) and a new prototype of solid-state flexible supercapacitor based on hydrogel electrodes (b).

## 2. Experimental section

### 2.1 Materials

Aniline (J&K Scientific.) was distilled before being used. Phytic acid, ammonia persulfate (APS) and polyvinyl alcohol (PVA) were bought from Alfa-Aesar, which were directly used as received without further purification. Carbon fiber cloths were purchased from CeTech Co. Ltd. (Taiwan), which were immersed in 6 M HNO<sub>3</sub> solution for overnight followed by washing with water, ethanol and acetone, drying in the oven at 60 °C and 20 min UV-ozone treatment.

### 2.2 Synthesis and characterization of PANI hydrogel

PANI hydrogel was synthesized according to the literature.<sup>22</sup> In a typical process, solution A was prepared by dissolving 143 mg (0.625 mmol) APS in 500  $\mu$ L DI water. Then, 229  $\mu$ L (2.5 mmol) aniline and 510  $\mu$ L (0.5 mmol) phytic acid (45%, wt / wt in water) were dissolving in 1000  $\mu$ L DI water to form solution B. The solution A and B were cooled to 4 °C in a refrigerator and then mixed quickly. In order to remove excess ions and oligomer, the PANI hydrogel was transferred into dialysis bag and purified for 5 days in DI water.

The formation of the PANI hydrogel was examined by tube-inversion method. Prior to morphologies and chemical structure characterization, the PANI hydrogel was transferred into a vacuum oven at 60 °C for overnight to form dehydrated PANI hydrogel. The morphologies of the dehydrated PANI hydrogel was checked using field emission scanning electron microscopy (FESEM, SIGMA, ZEISS). Fourier transform infrared spectroscopy (FTIR) and Ultraviolet-visible spectroscopy (UV-vis) were obtained by Spectrum One and PE Lambda 650/850/950, respectively. X-Ray diffraction (XRD) data was collected on a D8 Advance X-ray diffractometer (Bruker) with Cu K $\alpha$  radiation. Brunauer-Emmett-Teller (BET) surface area of the dehydrated PANI hydrogel was checked on a Micromeritics ASAP 2020 HD Analyzer.

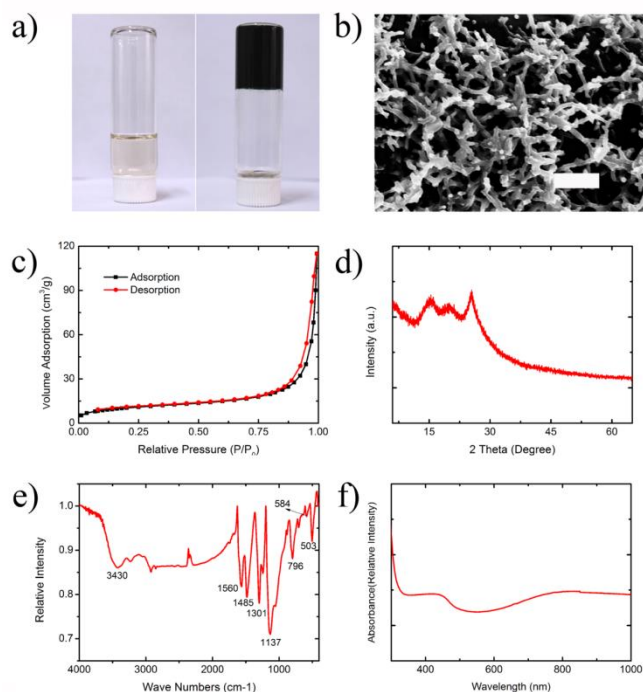


Figure 2 (a) Tube inversion examination of PANI hydrogel: a mixture of ANI and phytic acid aqueous solution before (left) and after adding APS oxides (right); (b) SEM images of dehydrated PANI hydrogel, the scale bar is 1  $\mu$ m; (c) Nitrogen adsorption-desorption isotherm of dehydrated PANI hydrogel; (d), (e) and (f) are XRD pattern, IR and UV-vis spectrum of dehydrated PANI hydrogel, respectively.

### 2.3 Preparation of the PANI hydrogel electrodes and common PANI nanowire electrodes

Carbon fiber cloth (CFC) was used as the three-dimension current collector due to its excellent electric conductivity and flexibility. During the synthesis process of the PANI hydrogel, the solutions A and B were mixed and immediately dropped onto the carbon cloths (coating area of 2 cm  $\times$  2 cm). After reacting for 6 h, the carbon fiber cloth supported PANI hydrogel was immersed into DI water for 24 h to remove the excess ions and oligomer.

In order to compare the performance of PANI hydrogel electrode with common PANI nanostructure electrode, a CFC supported PANI nanowire electrode was also prepared. Aniline (183  $\mu$ L, 2 mmol) was added to 40 mL of 0.5 M HClO<sub>4</sub> aqueous solution, and carbon fiber cloth (3 cm  $\times$  2 cm) was placed in the above solution. Ammonium persulfate (304 mg, 1.34 mmol) was added to the reaction solution at 0–5 °C and stirred. After reaction for 12 h, the carbon fiber cloth was removed and washed with deionized water.

### 2.4 Device preparation and electrochemical Performance tests

The electrochemical properties of PANI hydrogel electrode and common PANI nanowire electrode were characterized with both three-electrode and two-electrode setup. In a three-electrode apparatus, CFC supported PANI hydrogel was directly used as working electrode, a saturated calomel electrode (SCE) and a platinum plate were used reference and counter electrode, respectively. The electrolyte was 1M H<sub>2</sub>SO<sub>4</sub> aqueous solution.

A flexible solid-state supercapacitor was also fabricated with  $\text{H}_2\text{SO}_4/\text{PVA}$  hydrogel as the electrolyte. The  $\text{H}_2\text{SO}_4/\text{PVA}$  hydrogel was prepared by mixing 2g concentrated  $\text{H}_2\text{SO}_4$  and 2g PVA in 20mL DI water and heated at  $85^\circ\text{C}$  under vigorous stirring until the solution became clear. Two CFC supported PANI hydrogel electrodes and a filter paper (that was used as separator) was soaked in the  $\text{H}_2\text{SO}_4/\text{PVA}$  solution and then was solidified in the oven at  $50^\circ\text{C}$  for 30 mins. Finally, two electrodes and the filter paper filling with gel electrolytes were stacked together with a series of PANI electrode - filter paper - PANI electrode.

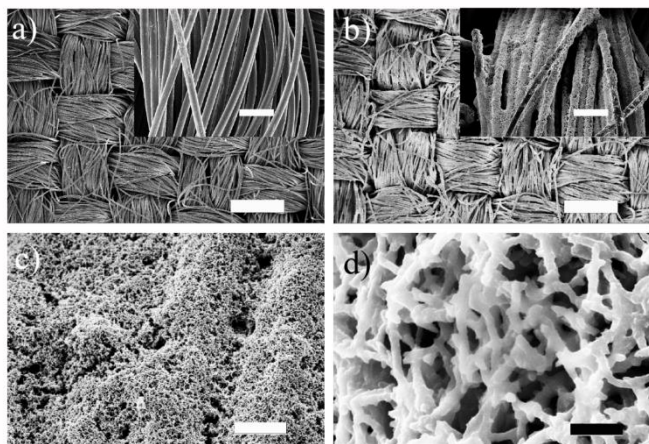


Figure 3 Morphologies of CFC and PANI hydrogel coated CFC obtained by SEM examination: (a) CFC (the scale bar is 400  $\mu\text{m}$ ); the insert image is the enlarged SEM images that shows the CFC is composed of carbon fibers (the scale bar is 40  $\mu\text{m}$ ). (b) Dehydrated PANI hydrogel coated CFC (the scale bar is 400  $\mu\text{m}$ ); the insert image is the enlarged SEM images (the scale bar is 40  $\mu\text{m}$ ), which shows the PANI hydrogel are coated on CFC surface completely. (c) and (d) are enlarged dehydrated PANI hydrogel morphologies on CFC surface (the scale bar is 4  $\mu\text{m}$  and 400 nm, respectively) that exhibits the 3D porous structure of PANI hydrogel.

Cyclic voltammetry (CV), electrochemical impedance spectroscopy (EIS) tests were performed with a CHI (660C) electrochemical workstation. In order to evaluate the charge-discharge cyclic stability of the PANI hydrogel based supercapacitors, Galvanostatic charge-discharge (GCD) measurements were carried out on a Arbin battery tester.

### 3. Results and discussion

#### 3.1 Synthesis and characterization of PANI Hydrogel

In the formation process of PANI hydrogel, a polyhydroxy acid called phytic acid is used as cross-linker according to the literature.<sup>22</sup> As we know, PANI is normally synthesized via oxidation polymerization from aniline monomers with dopants.<sup>20, 23</sup> In order to synthesize conducting polymer hydrogel, phytic acid is used as dopant. Each phytic acid molecular contains several phosphorous groups which protonate the nitrogens of PANI chains, thus, each phytic acid molecular can interact with more than one PANI molecular chain. Therefore, phytic acid crosslinks the PANI chain and further cause the gelation of PANI. In another word, phytic acid is actually like a gelator. The synthesis process is quite fast which just need around 3min. We use tube inversion method

that is a commonly used examination method to check the formation of the PANI hydrogel. The left image in Figure 2a is the transparency reaction solution (aniline and phytic acid mixture aqueous solution), and this solution lost the liquid mobility when APS was added (the right picture of Figure 2a), which confirms that the PANI hydrogel was formed. After removing the excess ions and oligomer by dialysis in the DI water for 5 days, the purified PANI hydrogel was dried in the vacuum oven at  $60^\circ\text{C}$  for 12 hours to form dehydrated PANI hydrogel for the morphology and chemical

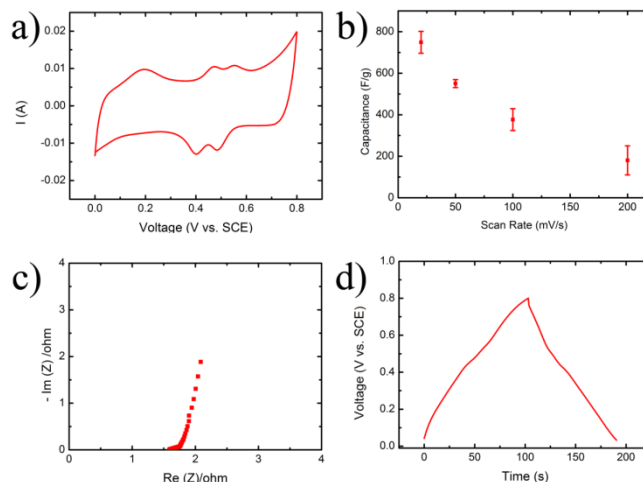


Figure 4 Electrochemical measurements of PANI hydrogel electrode with three-electrode apparatus: (a) CV curves at a scanning rate of 5mV/s; (b) Capacitance plots as the scanning rates increasing based on five batch of samples; (c) EIS data with a frequency range of 100 KHz to 1Hz at open-circuit potential; (d) Galvanostatic charge – discharge curve at 10 mA.

structure characterization. Scanning electron microscopy (SEM) was used to investigate the micro-structure of PANI hydrogel. From Figure 2b, the dehydrated PANI hydrogel is three-dimension interconnected PANI networks like porous foam, which is a typical hydrogel mesh-like micro-structure. The diameter of the mesh-like PANI nanofiber is around 100 nm. The PANI hydrogel can be swollen in the DI water with a high water content (*c.a.* 93%), which is favorable for ions diffusion, especially for the electrolyte ions diffusing into the inside of electrode in a supercapacitor.<sup>21</sup>

As the PANI hydrogel possesses porous micro-structure, the Brunauer–Emmett–Teller (BET) adsorption-desorption measurement was also performed to check the specific surface area (SFA) of dehydrated PANI hydrogel as shown in Figure 2c. According to the BET test, the SFA of the dehydrated PANI hydrogel is  $35\text{ m}^2\text{ g}^{-1}$ , which was comparable with other chemically synthesized PANI nanostructure.<sup>24, 25</sup> Figure 2d shows the XRD pattern of dehydrated PANI hydrogel. The peaks located at around  $2\theta = 16.0^\circ$  and  $20.0^\circ$  are attributed to periodicity paralleling to the polymer chains, while the intensity peak centered at  $2\theta = 25.0^\circ$  is corresponding to the periodicity perpendicular to the polymer chains ( $\pi - \pi$  stacking).<sup>26, 27</sup> All these peaks show the dehydrated PANI hydrogel is partially crystalline consisted with previous literature data.<sup>22</sup>

FTIR and UV-vis were used to analyze the chemical structure of the PANI hydrogel. In the FTIR spectrum (Figure 2e), the band observed at  $3430\text{ cm}^{-1}$  is generally due to N - H stretching of the primary amines. The characteristic adsorption at 1560

and  $1485\text{ cm}^{-1}$  are ascribed to the C = C stretching deformation of quinoid ring and benzenoid ring, respectively, which reveals that the chemical structure of PANI hydrogel is emeraldine instead of leucoemeraldine or permigraniline state.<sup>24</sup> The peaks at  $1301\text{ cm}^{-1}$  derives from C - N stretching vibration of primary aromatic amines. The characteristic absorption around  $1137\text{ cm}^{-1}$  is assigned to doped state of PANI. The peaks around  $796$  and  $503\text{ cm}^{-1}$  is normally due to the C - H bending vibrations within the 1, 4 - disubstituted aromatic ring. Besides, the purified PANI hydrogel after dialysis was further dispersed into DI water to form solution for UV-vis examination. In UV - vis spectrum of Figure 2f, the characteristic bands at  $430\text{ nm}$  and the long tail (free carrier tail) at wavelength longer than  $800\text{ nm}$  are assigned to polaron -  $\pi$  transition, which further confirms the chemical structure of PANI hydrogel is the doped emeraldine state.<sup>27</sup>

### 3.2 Electrochemical performance of PANI Hydrogel electrode

In order to analyze the electrochemical properties, the PANI hydrogel was in-situ coated on the surface of carbon fiber non-woven cloth that has three-dimension structure and excellent electric conductivity. In this case, a carbon fiber cloth (CFC) supported PANI hydrogel electrode was prepared without binder, which could be directly carried out electrochemical measurements with three-electrode system or made a supercapacitor. Figure 3a shows the morphologies of the carbon fiber non-woven cloth, which is comprised of 3D carbon fibers as seen in the insert image of the Figure 3a. During the synthesis process of the PANI hydrogel (see experimental part), the reaction solutions A and B were mixed and immediately dropped onto a  $2\text{ cm} \times 3\text{ cm}$  square carbon cloth (the coating area of  $2\text{ cm} \times 2\text{ cm}$ ). After reacting for 6 h, the CFC supported PANI hydrogel was immersed into DI water for 24 h to remove the excess ions, acid and oligomer. Figure 3b is the SEM image of PANI hydrogel coated CFC, which clearly shows a layer of coating on the CFC surface. From the insert image in Figure 3b, the surface of carbon fibers is covered completely by PANI hydrogel. Figure 3c and d are the enlarged SEM images of PANI hydrogel coated on CFC, which shows the PANI hydrogel possesses obvious porous foam structure. Three-electrode setup with  $1\text{ M H}_2\text{SO}_4$  aqueous as electrolyte was used to characterize the electrochemical properties of the single PANI hydrogel electrode. The CFC supported PANI hydrogel was directly used as the working electrode. Cyclic voltammetry (CV) with the potential range of  $0 - 0.8\text{ V}$  was recorded at  $5\text{ mV/s}$  as seen in the Figure. 4a. The typical redox characteristic peaks could be observed, which are ascribed to the transformation between leucoemeraldine base (LB), emeraldine salt (ES) and pernigraniline base (PB).<sup>28</sup> In order to check the rate capability of the PANI hydrogel electrode, the CVs with different scanning rates were carried out (Figure S1). According to the CV curves, the specific capacitance of the PANI hydrogel could be calculated as shown in Figure 4b. The capacitance plots at different scanning rates ( $20, 50, 100,$  and  $200\text{ mV/s}$ ) is obtained based on five batch of PANI electrode samples. The capacitance of the PANI hydrogel electrode at  $20\text{ mV/s}$  is around  $750\text{ F/g}$ , where the loading weight of PANI hydrogel is  $0.5\text{ mg/cm}^2$  (dry weight). Even the scanning rate increases to  $200\text{ mV/s}$  (10 times larger than  $20\text{ mV/s}$ ), the capacitance can still get  $200\text{ F/g}$  which exhibits the superior rate capability of the PANI hydrogel electrode. From the electrochemical impedance spectroscopy (EIS) in Figure 4c, the equivalent series resistance (ESR) extracted from high

frequency ( $100\text{ kHz}$ ) is around  $1.6\Omega$ , which means only very low ohmic contact present in the test system.<sup>29</sup> Galvanostatic charge-discharge (GCD) was also performed to evaluate the electrochemical performance of the PANI hydrogel electrode at  $10\text{ mA}$  (c.a.  $6\text{ A/g}$ ), shown in the Figure. 4d. Cyclic stability was tested by GCD tests at  $40\text{ mA}$ , and the capacitance retain plots was given in Figure S2. After  $1000$  GCD cycles, the capacitance could be kept at  $80\%$ , which is a comparable cyclic stability compared with other PANI nanostructure in the literature.<sup>30-32</sup> In order to sufficient know the performance of PANI hydrogel electrode, we also prepared CFC supported common PANI nanowire electrode as benchmark sample (Figure S2). This PANI benchmark electrode possesses nanowire structure with a diameter of c.a.  $100\text{ nm}$  according to Figure S3a. Moreover, the electrochemical properties of PANI hydrogel electrode and common PANI nanowire electrode were characterized by CV measurements as seen as in (Figure S3b). Specific capacitance plots of both electrodes at different scanning rates and at different current densities are obtained based on CVs and GCD tests, respectively. From Figure S3c and Figure S3d, the capacitance of the PANI hydrogel electrode is obviously better than common PANI nanowire electrode.

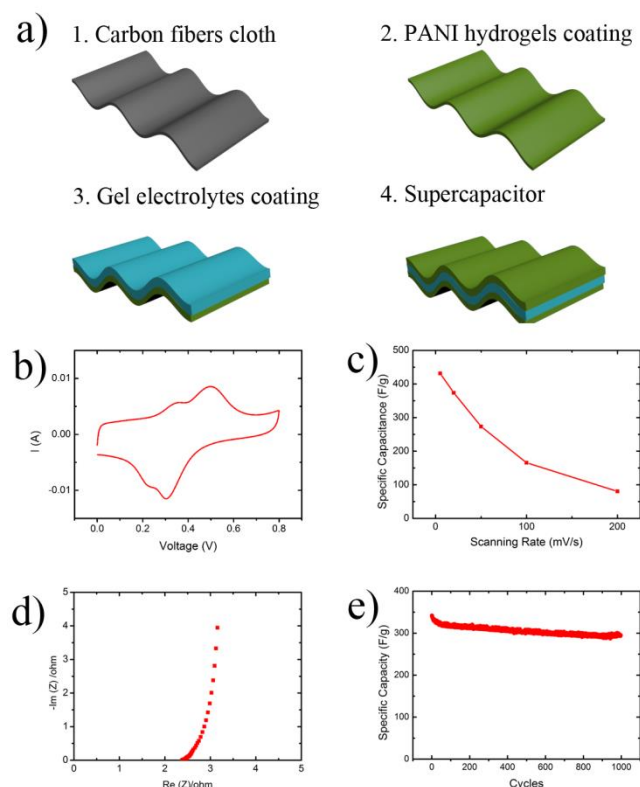


Figure 5 (a) Schematic of preparation process of PANI Hydrogel based solid-state supercapacitors; (b) CV curves at a scanning rate of  $5\text{ mV/s}$ ; (c) Capacitance plots as the scanning rates; (d) EIS data with a frequency range of  $100\text{ KHz}$  to  $1\text{ Hz}$  at open-circuit potential; (e) Capacitance retention plot obtained from galvanostatic charge – discharge tests at  $7.5\text{ A/g}$

### 3.3 Flexible solid-state supercapacitors prototype based on PANI Hydrogel electrodes

A flexible solid-state supercapacitor was fabricated based on CFC supported PANI hydrogel electrodes and  $\text{H}_2\text{SO}_4/\text{PVA}$  gel - polymer electrolytes. Gel - polymer electrolytes that have high

physical flexibility and remarkable electrochemical properties are widely used in solid-state supercapacitors. In this paper, the CFC supported PANI hydrogel materials instead of traditional solid electrode materials were active electrode materials to make the flexible supercapacitors. The detailed fabrication process is described in experimental part, and schemed in Figure 5a. The electrochemical performance of the as-prepared supercapacitor devices with symmetric two-electrode configuration were measured. Figure 5b is the CV curve of device at a scanning rate of 5 mV/s with the potential window of 0-0.8V, which shows the different shape with that in three-electrode system that was consisted with previous literature.<sup>33, 34</sup> Besides, the CVs at different scanning rates were also recorded (Figure S4) and the capacitance plots following the scanning rates change were calculated and shown in the Figure 5c. According to the plots, the capacitance at a scanning rate of 5 mV/s is 430 F/g calculated based on the dried weight of PANI hydrogel. In a PANI based flexible solid-state supercapacitor with two-electrode configuration, the capacitance (430 F/g) for PANI electrode is larger than most previous literature.<sup>13, 35-37</sup> It is proposed that the unique hydrogel structure of the PANI electrode brings this superior capacitance performance. Generally, the pseudocapacitance of the conducting polymers comes from the redox reactions occurring near the surface of active materials.<sup>32</sup> A larger interfacial contact between the electrode and the electrolyte solution results in more efficient electrochemical processes and thus the larger capacitance.<sup>38-40</sup> In the case of solid-state electrode, the gel electrolytes are basically hard to diffuse into the inside of the solid electrode due to large viscosity. Therefore the inner active materials cannot contact with electrolytes completely. However, PANI hydrogel electrode materials employed in this research possess a 3D hierarchical porous nanostructure swelling with liquid that facilitate ions and mass transport which makes inner active materials accessible to electrolytes and led to the large capacitance. From EIS plot in Figure 5d, it shows a typical capacitive characteristic that means the as-prepared device is a well-fabricated supercapacitor. The ESR at high frequency (100 kHz) is around 2.3  $\Omega$ , which shows this solid-state device has only very low ohmic resistance compared with previously reported solid - state supercapacitors.<sup>31, 41-43</sup> In order to study the cycle life under consecutive charge-discharge cycles of the device, galvanostatic charge-discharge measurements were carried out at 7.5 A/g with a potential window of 0-0.8 V (Figure S5). The capacitance decay plot was shown in Figure 5e. After 1000 consecutive charge-discharge cycles, the capacitance still can keep 86% compared with the original capacitance that is higher than that in three-electrode aqueous system (80%). The improvement in cyclic stability is proposed to be due to the quasi-solid-state gel electrolytes which could further protect active PANI and avoid the PANI delamination from current collector.

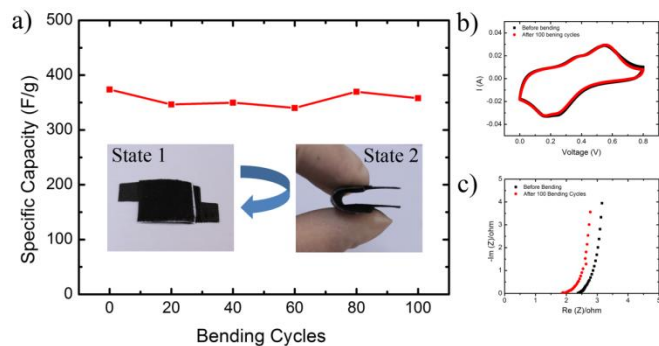


Figure 6 In-situ flexibility tests of the PANI hydrogel based supercapacitors: (a) Capacitance retention plot under bending cycles increase; one bending cycle means that the supercapacitor starts from state 1 (insert image), going state 2 (insert image) and going back to state 1; (b) and (c) are CV curves and EIS data before bending tests and after 100 bending cycles.

As a flexible supercapacitor, it should possess excellent flexibility without sacrificing their electrochemical performance. The electrochemical performance of our device under bending state was evaluated using an in - situ measuring method. Figure 6a is the capacitance retaining plots following the bending cycle increase, which derived from their CV curves at a constant scanning rate of 20 mV/s after bending. From the insert image of Figure 6a, one bend cycle starts from state 1, passing state 2(bending angle is 180°) and then going back to state 1. According to the experiments, the capacitance of device is maintained very well even after one hundred bending cycles. From Figure 6 b, no obviously change were found in the CV curves before bend cycling and after one hundred bend cycles. From EISs measurements as shown in Figure 6c, the ESR of device is even reduced after 100 bend cycles, which means the contact between different layers of device becomes better after bend cycling instead of deterioration. All these bending tests were performed using only one device, showing that the supercapacitor has remarkable bendable performance.

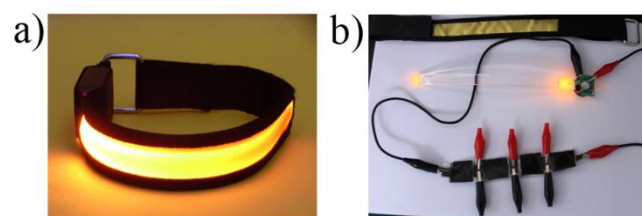


Figure 7 (a) A glow armlet that is normally worn for safety warning by the people who like jogging at nightfall is driven by two commercial coin batteries; (b) It was driven by four as-prepared PANI hydrogel based solid-state flexible supercapacitors connected in series.

To demonstrate if the as-prepared device works, a fashion glow armlet that is normally worn for safety warning by the people who like jogging at nightfall was driven by our devices. The glow armlet is generally driven by two serial - connected lithium manganese coin batteries (CR2032) as shown in Figure 7a. We took out the original lithium batteries from the glow armlet and just used our devices to drive it. Four as-prepared supercapacitor devices were connected in series using alligator clips to form the power sources unit. After being charged by two AA batteries (3V) for 10 seconds, the serial-connected devices can drive the glow armlet work for several minutes as shown in Figure 7b, which exhibits the as-prepared supercapacitor works very well in a real application.

#### 4. Conclusions

In this paper, PANI hydrogel is used as active electrode material to make a flexible solid-state supercapacitor, which exhibits superior electrochemical performance. Conducting

polymer hydrogel combines the unique properties of hydrogel with the electrical properties, thus offering intrinsic 3D porous conducting frameworks and promoting the transport of charges, ions, and molecules. The morphology, chemical structure and electrochemical properties of the single PANI hydrogel electrode were characterized in system. PANI hydrogel electrode materials are 3D hierarchical porous nanostructure and are swelling with aqueous solution that improves the contact between electrode and electrolytes which bring the large capacitance in a solid-state supercapacitors. The capacitance of the PANI hydrogel is 430F/g in the solid-state supercapacitor, which is almost the largest capacitance obtained in a solid-state supercapacitor with two-electrode system based on PANI. Furthermore, this supercapacitor shows excellent bendable performance. The capacitance is almost no any decay after one hundred bend cycles. This device can drive a glow armlet to work for several minutes after being charged for just 10 seconds, which demonstrates the device fabricated here is highly promising in the case of real application.

## Acknowledgements

The authors thank the fund support by National Natural Science Foundation of China (Grants 51403211 and 51472238), and start funding support from the Institute of Electrical Engineering, Chinese Academy of Sciences.

## Notes and references

Institute of Electrical Engineering, Chinese Academy of Sciences, Beijing, 100190, China.

E-mail: ywma@mail.iee.ac.cn; wangkai@mail.iee.ac.cn

† Electronic Supplementary Information (ESI) available: the detailed electrochemical measurements data of PANI hydrogel electrodes, such as CVs, galvanostatic charge-discharge and cyclic stability]. See DOI: 10.1039/b000000x/

1. B. S. Shim, W. Chen, C. Doty, C. L. Xu and N. A. Kotov, *Nano Lett.*, 2008, **8**, 4151-4157.
2. S. Park and S. Jayaraman, *MRS Bull.*, 2003, **28**, 585-591.
3. K. Jost, G. Dion and Y. Gogotsi, *J. Mater. Chem. A*, 2014, **2**, 10776-10787.
4. X. F. Wang, X. H. Lu, B. Liu, D. Chen, Y. X. Tong and G. Z. Shen, *Adv. Mater.*, 2014, **26**, 4763-4782.
5. S. Y. Lee, K. H. Choi, W. S. Choi, Y. H. Kwon, H. R. Jung, H. C. Shin and J. Y. Kim, *Energy Environ. Sci.*, 2013, **6**, 2414-2423.
6. H. Gwon, J. Hong, H. Kim, D. H. Seo, S. Jeon and K. Kang, *Energy Environ. Sci.*, 2014, **7**, 538-551.
7. D. P. Dubal, J. G. Kim, Y. Kim, R. Holze, C. D. Lokhande and W. B. Kim, *Energy Technol.*, 2014, **2**, 325-341.
8. G. M. Zhou, F. Li and H. M. Cheng, *Energy Environ. Sci.*, 2014, **7**, 1307-1338.
9. B. E. Conway, *Electrochemical Supercapacitors, Scientific Fundamentals and Technological Applications*, Kluwer Academic/Plenum New York, 1999.
10. L. P. Wang, L. H. Yu, R. Satish, J. X. Zhu, Q. Y. Yan, M. Srinivasan and Z. C. Xu, *RSC Adv.*, 2014, **4**, 37389-37394.
11. P. Simon and Y. Gogotsi, *Nat. Mater.*, 2008, **7**, 845-854.
12. C. Wei, P. S. Lee and Z. C. Xu, *RSC Adv.*, 2014, **4**, 31416-31423.
13. K. Wang, H. P. Wu, Y. N. Meng and Z. X. Wei, *Small*, 2014, **10**, 14-31.
14. N. A. Choudhury, S. Sampath and A. K. Shukla, *Energy Environ. Sci.*, 2009, **2**, 55-67.
15. Y. Lu, W. N. He, T. Cao, H. T. Guo, Y. Y. Zhang, Q. W. Li, Z. Q. Shao, Y. L. Cui and X. T. Zhang, *Sci Rep*, 2014, **4**.
16. R. Fuhrer, E. K. Athanassiou, N. A. Luechinger and W. J. Stark, *Small*, 2009, **5**, 383-388.
17. S. B. Ye and J. C. Feng, *ACS Appl. Mater. Interfaces*, 2014, **6**, 9671-9679.
18. Y. Shi, L. J. Pan, B. R. Liu, Y. Q. Wang, Y. Cui, Z. A. Bao and G. H. Yu, *J. Mater. Chem. A*, 2014, **2**, 6086-6091.
19. S. Ghosh and O. Ingnas, *Adv. Mater.*, 1999, **11**, 1214-1218.
20. D. Li, J. X. Huang and R. B. Kaner, *Accounts Chem. Res.*, 2009, **42**, 135-145.
21. Y. Zhao, B. R. Liu, L. J. Pan and G. H. Yu, *Energy Environ. Sci.*, 2013, **6**, 2856-2870.
22. L. J. Pan, G. H. Yu, D. Y. Zhai, H. R. Lee, W. T. Zhao, N. Liu, H. L. Wang, B. C. K. Tee, Y. Shi, Y. Cui and Z. N. Bao, *Proc. Natl. Acad. Sci. U. S. A.*, 2012, **109**, 9287-9292.
23. W. S. Huang, B. D. Humphrey and A. G. Macdiarmid, *Journal of the Chemical Society-Faraday Transactions I*, 1986, **82**, 2385-&.
24. M. R. Gizdavic-Nikolaidis, M. Jevremovic, D. R. Stanislavljev and Z. D. Zujovic, *J. Phys. Chem. C*, 2012, **116**, 3235-3241.
25. J. X. Huang and R. B. Kaner, *J. Am. Chem. Soc.*, 2004, **126**, 851-855.
26. Z. X. Wei, Z. M. Zhang and M. X. Wan, *Langmuir*, 2002, **18**, 917-921.
27. J. J. Xu, K. Wang, S. Z. Zu, B. H. Han and Z. X. Wei, *ACS Nano*, 2010, **4**, 5019-5026.
28. K. Wang, J. Y. Huang and Z. X. Wei, *J. Phys. Chem. C*, 2010, **114**, 8062-8067.
29. R. Kotz and M. Carlen, *Electrochim. Acta*, 2000, **45**, 2483-2498.
30. K. Wang, P. Zhao, X. M. Zhou, H. P. Wu and Z. X. Wei, *J. Mater. Chem.*, 2011, **21**, 16373-16378.
31. K. Wang, Q. H. Meng, Y. J. Zhang, Z. X. Wei and M. H. Miao, *Adv. Mater.*, 2013, **25**, 1494-1498.
32. G. A. Snook, P. Kao and A. S. Best, *J. Power Sources*, 2011, **196**, 1-12.
33. V. Khomenko, E. Frackowiak and F. Beguin, *Electrochim. Acta*, 2005, **50**, 2499-2506.
34. M. D. Stoller and R. S. Ruoff, *Energy Environ. Sci.*, 2010, **3**, 1294-1301.
35. C. Z. Meng, C. H. Liu, L. Z. Chen, C. H. Hu and S. S. Fan, *Nano Lett.*, 2010, **10**, 4025-4031.
36. Q. Wu, Y. X. Xu, Z. Y. Yao, A. R. Liu and G. Q. Shi, *ACS Nano*, 2010, **4**, 1963-1970.
37. Y. N. Meng, K. Wang, Y. J. Zhang and Z. X. Wei, *Adv. Mater.*, 2013, **25**, 6985-6990.

38. P. Si, S. J. Ding, X. W. Lou and D. H. Kim, *RSC Adv.*, 2011, **1**, 1271-1278.
39. J. Y. Huang, K. Wang and Z. X. Wei, *J. Mater. Chem.*, 2010, **20**, 1117-1121.
40. L. Yu, Z. Y. Wang, L. Zhang, H. B. Wu and X. W. Lou, *J. Mater. Chem. A*, 2013, **1**, 122-127.
41. K. Wang, H. P. Wu, Y. N. Meng, Y. J. Zhang and Z. X. Wei, *Energy Environ. Sci.*, 2012, **5**, 8384-8389.
42. K. Wang, W. J. Zou, B. G. Quan, A. F. Yu, H. P. Wu, P. Jiang and Z. X. Wei, *Adv. Energy Mater.*, 2011, **1**, 1068-1072.
43. X. H. Lu, Y. X. Zeng, M. H. Yu, T. Zhai, C. L. Liang, S. L. Xie, M. S. Balogun and Y. X. Tong, *Adv. Mater.*, 2014, **26**, 3148-3155.